

constant or rise rather than fall between rows 6 and 7. A flat trend would give  $\Delta H_v$ 's of 40 to 45 kcal/mole for elements 113 to 115, approaching the required value for G.

Of the remaining volatile elements, 112 and 116 to 119, the last three can probably be excluded. Elements 117 and 118 can be ruled out because  $^{136}\text{Xe}_f$  does not correlate either in abundance or in thermal release pattern with  $^{129}\text{Xe}$  (from the decay of extinct  $^{129}\text{I}$ ), or with primordial  $^{132}\text{Xe}$  (I, 14). Thus its progenitor apparently was not a halogen or noble gas, otherwise it would have been trapped at the same sites. Element 119, ekafrancium, cannot be excluded on chemical grounds because its heaviest stable congener, Cs, has an abundance pattern in meteorites similar to that of other volatile elements (II). No calculations are possible, because the host phase and solid-solution behavior of Cs are not known. The principal argument against element 119 thus is its short predicted  $\alpha$ -decay half-life, about 1 second.

The remaining two elements, 112 and 116, probably form stable Ni compounds in the solar nebula, by analogy with their lighter congeners Hg and Po. Judging from the meteoritic abundances of Hg, Te, and Se (16), their condensation temperatures seem to have been raised into the 400° to 700°K range, probably by compound formation. Significantly, these elements do not show the steep drop of abundance with accretion temperature that is characteristic of  $^{136}\text{Xe}_f$  and the insoluble metals of groups 3B to 5B, In, Tl, Pb, and Bi (Fig. 1). Presumably the 2B and 6B elements are more soluble in major meteoritic phases, such as Ni-Fe or FeS. If this trend extends into the region of superheavy elements, 112 and 116 must be rated among the less likely choices.

Thus the principal candidates are 111 and 115, followed by 113, 114, 112, and 116 in that order. This choice is based on the apparent volatility of the free element; to narrow the range further, it will be necessary to establish its oxidation state and chemical behavior, by appropriate studies on meteorites.

EDWARD ANDERS

*Enrico Fermi Institute and  
Department of Chemistry,  
University of Chicago,  
Chicago, Illinois 60637*

JOHN W. LARIMER

*Department of Geology, Arizona  
State University, Tempe 85281*

#### References and Notes

- J. H. Reynolds and G. Turner, *J. Geophys. Res.* **69**, 3263 (1964); C. M. Hohenberg, M. N. Munk, J. H. Reynolds, *ibid.* **72**, 3139 (1967); M. W. Rowe, *Geochim. Cosmochim. Acta* **32**, 1317 (1968); J. H. Reynolds, in *Recent Developments in Mass Spectroscopy*, K. Ogata and T. Hayakawa, Eds. (Univ. of Tokyo Press, Tokyo, 1970), p. 594.
- M. W. Rowe and P. K. Kuroda, *J. Geophys. Res.* **70**, 709 (1965).
- G. J. Wasserburg, J. C. Huneke, D. S. Burnett, *Phys. Rev. Lett.* **22**, 1198 (1969).
- E. C. Alexander Jr., R. S. Lewis, J. H. Reynolds, M. C. Michel, *Science* **172**, 837 (1971).
- F. A. Podosek, *Earth Planet. Sci. Lett.* **8**, 183 (1970).
- E. Anders and D. Heymann, *Science* **164**, 821 (1969).
- A. G. W. Cameron, *Earth Planet. Sci. Lett.* **1**, 93 (1966); F. L. Whipple, *Science* **153**, 54 (1966); J. W. Larimer and E. Anders, *Geochim. Cosmochim. Acta* **31**, 1239 (1967).
- O. Eugster, P. Eberhardt, J. Geiss, *Earth Planet. Sci. Lett.* **3**, 249 (1967); K. Marti, *ibid.*, p. 243; R. O. Pepin, in *Origin and Distribution of the Elements*, L. H. Ahrens, Ed. (Pergamon, Oxford, 1968), p. 379.
- M. Dakowski, *Earth Planet. Sci. Lett.* **6**, 152 (1969); B. Srinivasan, E. C. Alexander, Jr., O. K. Manuel, D. E. Troutner, *Phys. Rev.* **179**, 1166 (1969). See the following references for further information on superheavy elements: G. T. Seaborg, *Annu. Rev. Nucl. Sci.* **18**, 53 (1968); M. Dakowski, *Phys. Lett.*, in press; D. N. Schramm, *Nature* **233**, 258 (1971); — and W. A. Fowler, *ibid.* **231**, 103 (1971).
- W. R. Van Schmus and J. A. Wood, *Geochim. Cosmochim. Acta* **31**, 747 (1967).
- L. Anders, *Annu. Rev. Astron. Astrophys.* **9**, 1 (1971); in *From Plasma to Planet*, Proceedings of the 21st Nobel symposium (Almqvist and Wiksell, Stockholm, in press); R. Keays, R. Ganapathy, E. Anders, *Geochim. Cosmochim. Acta* **35**, 337 (1971); J. C. Laul, R. Ganapathy, E. Anders, J. W. Morgan, in preparation.
- N. Onuma, R. N. Clayton, T. K. Mayeda, *Geochim. Cosmochim. Acta*, in press; L. Grossman, *ibid.*, in press; M. S. Lancet, thesis, University of Chicago (1972).
- J. W. Larimer, *Geochim. Cosmochim. Acta* **31**, 1215 (1967); in preparation. In Eqs. 1 and 2, the slight temperature dependence of the heat and entropy of vaporization has been neglected. Hence, the curves in Fig. 1 fall 10° to 15° higher than they should (assuming that the  $\Delta H_s$  estimates are correct). This approximation has the advantage of permitting a direct comparison between known and unknown  $\Delta H_v$  values.
- D. Heymann and E. Mazor, *Geochim. Cosmochim. Acta* **32**, 1 (1968); O. Eugster, P. Eberhardt, J. Geiss, *J. Geophys. Res.* **74**, 3874 (1969); M. A. Reynolds, M. N. Rao, J. L. Meason, P. K. Kuroda, *ibid.*, p. 2711; E. Mazor, D. Heymann, E. Anders, *Geochim. Cosmochim. Acta* **34**, 781 (1970).
- A. G. W. Cameron, in *Origin and Distribution of the Elements*, L. H. Ahrens, Ed. (Pergamon, Oxford, 1968), p. 125.
- W. D. Ehmann and J. F. Lovering, *Geochim. Cosmochim. Acta* **31**, 357 (1967); G. W. Reed, Jr., and S. Jovanovic, *J. Geophys. Res.* **72**, 2219 (1967); —, in *Origin and Distribution of the Elements*, L. H. Ahrens, Ed. (Pergamon, Oxford, 1968), p. 321.
- R. A. Schmitt and R. H. Smith, in *Origin and Distribution of the Elements*, L. H. Ahrens, Ed. (Pergamon, Oxford, 1968), p. 283; S. N. Tandon and J. T. Wasson, *Geochim. Cosmochim. Acta* **32**, 1087 (1968).
- O. L. Keller, Jr., J. L. Burnett, T. A. Carlson, C. W. Nestor, Jr., *J. Phys. Chem.* **74**, 1127 (1970).
- Supported in part by AEC contract AT(11-1)-382.

15 October 1971; revised 20 December 1971 ■

## Infrared Spectral Emittance in Geological Mapping: Airborne Spectrometer Data from Pisgah Crater, California

*Abstract. Measurements of spectral emittance in the infrared region from 6.8 to 13.3 micrometers were made with an airborne spectrometer at a rate of six spectra per second, on flights 650 meters above the olivine basalt flows at Pisgah Crater in the southern Californian desert. The spectra show chemical and mineralogical differences that can be related to differences in the terrain below the aircraft.*

At a recent symposium (1, 2), two presentations were made of the techniques of independently performed geological mapping from the air, over the same terrain. This report emphasizes the nonimaging technique involving spectral measurements in the infrared from 6.8 to 13.3  $\mu\text{m}$  taken while flying at 650 m (2000 feet) above the olivine basalt flows and alluvium and dry lake beds (Lavic Lake) at Pisgah Crater, near Barstow, California. The instrumentation (3), includes a boresight camera by which one can relocate the ground track of the (7 mrad, 0.4°) circular field of view of the spectrometer (4).

A total of 514 of the 4300 spectra were collected (4) in four flight lines of total length 28 km (5). They were separated into 31 geological groupings, located as black and white bands on the large-scale photographs (Fig. 1) taken

at the same time along the flight line  $F-F'$  (6).

The raw radiance spectra from the rock and soil surfaces were ratioed by an average "water body" spectrum (average of 50 spectra) obtained by flying at the same altitude over a nearby lake (7). The emittance spectra were then inverted (8) and normalized for statistical studies, by setting their means at 0.0 and their standard deviation (S.D.) at 1.0. By this transform all the spectra have the same amplitude range, which permits more precise comparison of their information content. Care should be taken in using these normalized spectra, as they are no longer numerically the same as absolute emittance (used for calculating temperatures from radiance levels).

These selected spectra are then analyzed in two formats. In the first, emittance values for 10 to 50 spectra [mean

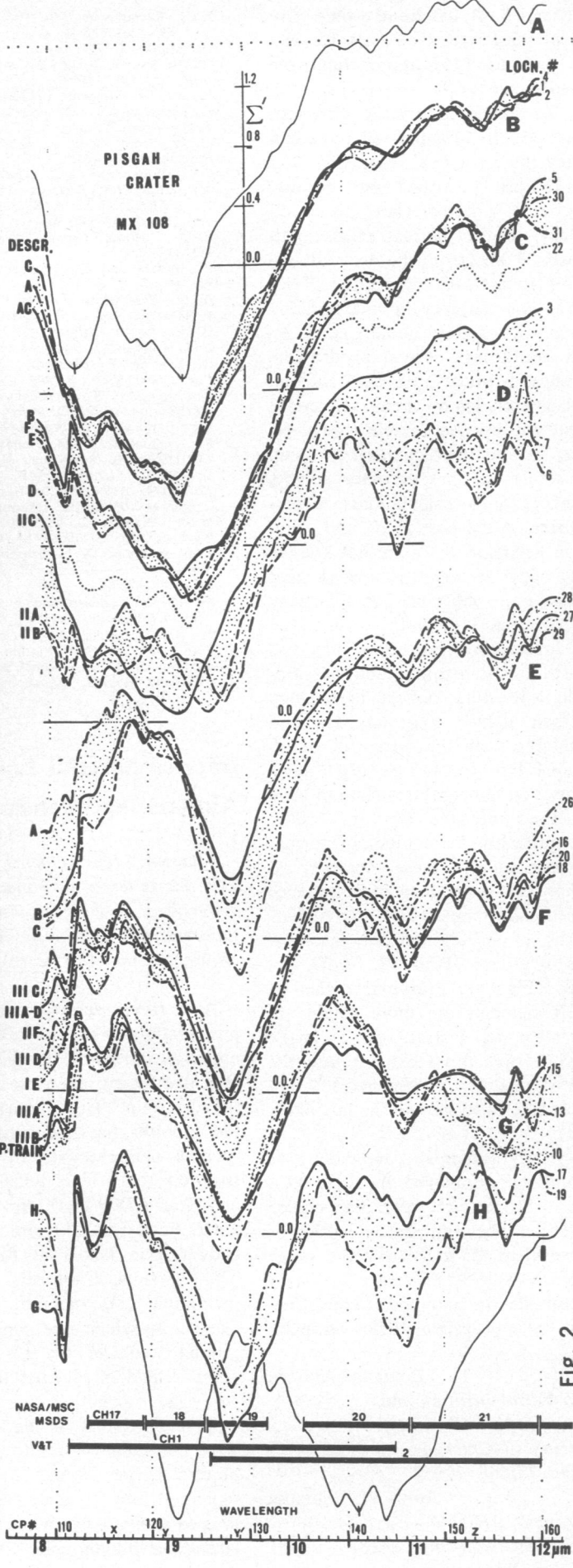
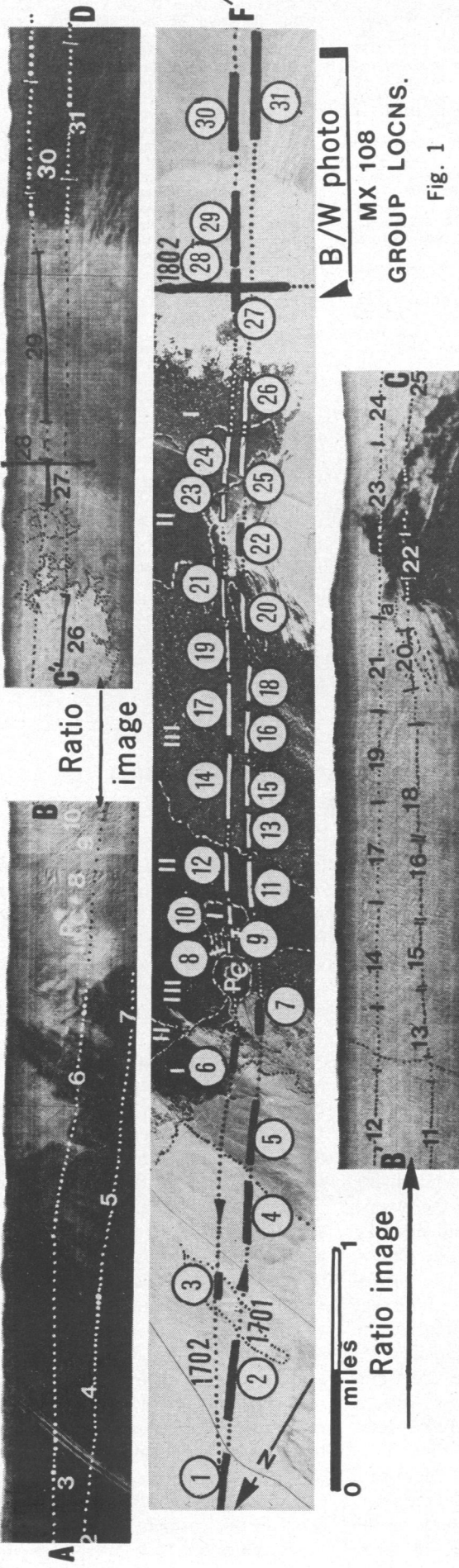


Fig. 1. Photograph of Pisgah Crater (PC), center, and three image strips (10); 1 mile = 1.6 km.

Fig. 2. Mean spectral emissance curves (11).

and  $\pm 1$  S.D.; (9)] are plotted as a function of wavelength. In the second, the standard deviations for 10 to 50 spectra are plotted in the same way. The standard deviation plot provides a rapid estimate of the variability of the data. It generally has one of two shapes, low and flat if there is little variability in radiance, or higher and bulging if there is considerable variability. An interesting standard deviation plot for the dry lake sediments of Lavic Lake (locality 28) shows a third type, with a pronounced upward bulge only where the reststrahlen effect (1-3, 10) indicated a chemical and mineralogical variation in an otherwise constant lake-floor terrain, which is clearly of geological significance.

The means of the spectral groups (or "mean spectra") may be compared by visual inspection, for example, by direct overlay of tracings (Fig. 2), or group populations may be studied by discriminant analysis (11). Several subgroups have been selected on the basis of more subtle features (such as weathering and surface chemical variability). In Fig. 2, B to H, the mean spectra of all the subgroups are plotted as single curves to show their similarities within a geological class. Thus, each spectrum represents the average of many individual spectra sequentially observed over the distance indicated by the bars on F-F' in Fig. 1.

The geology of the Recent lavas, rocks, and soils has been described (12, 13). The spectra can be correlated with geology and meaningful, systematic variations appear in the flight data. The spectra of the "younger" alluvium (Fig. 2B) and "older" alluvium (Fig. 2C) groups are similar, with a single, strong sloping minimum at 9.1 to 9.2  $\mu\text{m}$ . Detailed examination shows that the pattern in Fig. 2B is displaced to shorter wavelengths and that the shoulder at 9.5  $\mu\text{m}$  is absent, which indicates a higher quartz (sand) content in the younger materials (12). Comparable similarities are shown by the three olivine basalt flow types (Fig. 2, F to H), all of which show a single, sharp minimum at 9.45 to 9.55  $\mu\text{m}$ . The differences between the basalt spectral types were emphasized by separating the subgroups that showed a weak minimum at 10.97  $\mu\text{m}$  (Fig. 2, F and G) from those that had a pronounced feature there (Fig. 2H). A further separation was made by means of the broad pattern around 11.5 to 12.0  $\mu\text{m}$  (in Fig. 2, F is flatter there than G). Com-

parable spectra of (polished) granodiorite (Fig. 2A) and gabbro (Fig. 2I) specimens have been included to show the closer similarity of the basalt to the gabbro spectrum (14).

The most interesting group (Fig. 2D) represents spectra from areas (3, 6, and 7 in Fig. 1) where blown sand now rests (patchily) in depths greater than the optical depth for these silicates. Thus, where cover is complete the spectrum of sand (here equivalent to the younger alluvium, Fig. 2B) should appear; where it is not complete the basalt spectrum should be evident. Within the group in Fig. 2D, the spectral mean IIC (locality 3) shows the younger alluvium pattern, while IIA (locality 7) is most like the basalt spectra (type 2, Fig. 2F), which establishes the ability of the airborne system to discern variations in rock composition. This variability is also clear on the A-B section of the ratio-imagery in Fig. 1 (10).

The spectra of dry lake sediments (Fig. 2E) from Lavic Lake present an enigma. Although creamy white in color, these fine-grained clays (12) consistently yield spectra (15) similar to those of the type-2 basalt flows (see Fig. 2B and localities 27, 28, and 29 in Fig. 1). This was true in 1965 in ground measurements along the same line. The new airborne data now support the earlier (still unexplained) findings. Similar support is gained from the ratio-imagery of the same area observed by Vincent and Thomson (10). Therefore, three pieces of evidence point to the similarity of the clay spectra to those of the nearby olivine basalt.

In summary, (i) infrared emittance spectra taken from the air over geologically selected areas across the Pisgah Crater lava flows show similarities within (and contrasts between) the areas. The spectral differences can be used to separate the flows. (ii) Within the lava flows themselves spectral types can be defined that (at the moment) are not clearly related to the mapped flow stages (flows I, II, and III); that is, the spectra are subtly depicting some other parameter than that used to differentiate the three flows in the field and on aerial photographs. (iii) Windblown sand on basalt shows spectra of sand, but where sand patchily covers the flow in one resolution cell the spectra of both the sand and the basalt appear in a composite pattern. (iv) The spectra of the dry lake sediments of argillic silts superficially resemble those of the basalt

flows, but group variability in chemical and mineralogical composition is shown by the shapes of the standard deviation plots. (v) Each of these spectral similarities and differences may also be observed in the imagery prepared by ratioing concurrent radiance levels in two adjacent wavelength channels 2.5  $\mu\text{m}$  wide (10). This is significant, as imagery is more practical to use than spectral curves. What cannot be explained yet is that this occurred with overlapping band-pass filters of such width (8.1 to 10.9  $\mu\text{m}$  and 9.4 to 12.0  $\mu\text{m}$ ). These bands (Fig. 2) must represent the integration of all the spectral information within their bounds and express it as an average value, rather than show all the finer points of spectral differences evident on the curves. A more precise separation of rock types can be effected by using nonoverlapping or narrower bands, or both, even with the lowered signal-to-noise ratio incurred by the lessened energy throughput. Such a multichannel system as that being built for the National Aeronautics and Space Administration's aircraft program (16) can become a geological mapping tool.

R. J. P. LYON

School of Earth Sciences,  
Stanford University,  
Stanford, California 94305

#### References and Notes

1. R. K. Vincent and F. J. Thomson, in *Proceedings of the International Symposium on Remote Sensing of the Environment, 7th* (Univ. of Michigan Press, Ann Arbor, 1971), pp. 247-252.
2. R. J. P. Lyon, *ibid.*, p. 1449.
3. ———, *Econ. Geol.* **60**, 715 (1965); ——— and J. Patterson, *Proceedings of the International Symposium on Remote Sensing of the Environment, 6th* (Univ. of Michigan Press, Ann Arbor, 1970), p. 527; *Proceedings of the International Symposium on Remote Sensing of the Environment, 4th* (Univ. of Michigan Press, Ann Arbor, 1966), p. 213.
4. Spectra are taken at a rate of six per second, while the aircraft moves 15 m. The field of view of the spectrometer is small (7 mrad or 7 m/km altitude); at an altitude of 700 m the spectra are from patches 15 m long by 5 m wide. The spectrometer uses a circular variable filter as the dispersive element, with spectral resolution  $\lambda/\Delta\lambda = 100$ .
5. Flights were made on National Aeronautics and Space Administration Mission 108, 8 October 1968, over Pisgah Crater, California, about 61 km (35 miles) southeast of Barstow, San Bernardino County.
6. Self-organizing ("clustering") programs were extensively used with the older, noisy (earlier than mission MX-108) data but were not useful. The stepwise discriminant program BMD07M (University of California at Los Angeles biomedical series) was the most suitable, both for early grouping into "training" groups and in the subsequent processing of other "unknown" spectral data.
7. In processing, the spectral emittance of water is used and blackbody radiance at the lake temperature (from the onboard radiometer,  $\Delta\lambda$  is 10.375 to 12.1  $\mu\text{m}$ ), is modified by these values, until a "water body" spectrum is obtained. [See R. J. P. Lyon and A.

Marshall, *Inst. Electr. Electron. Eng. Trans. GE-9*, 131 (1971)]. The bands (6.8 to 7.9  $\mu\text{m}$ ) and (12.0 to 13.3  $\mu\text{m}$ ) are then "clipped off" as they contain information from atmospheric constituents and not geological (silicate) materials (3).

8. Both units chop the incoming radiance against an internal blackbody, set at 60°C (spectrometer) and 50° or 60°C (radiometer). The output voltages increase with lower target temperatures. Nonblackbody radiators have lower brightness temperatures (emittance at any wavelength is not equal to 1.0) at wavelengths of chemical interest (reststrahlen bands); thus, raw spectra have maxima of output voltage in these bands. Inverting the emittance data corrects this problem (7).
9. It is assumed that the distribution of the emittance values about their mean follows a normal distribution curve. See R. Hoffer, in *Laboratory for Agricultural Research (LARS) Bulletin 844* (Purdue Univ. Studies, West Lafayette, Indiana, 1968), chap. 3, pp. 68-71.
10. R. K. Vincent and F. J. Thomson, *Science* **175**, 986 (1972).
11. In Fig. 2, the group number is the left-hand symbol and the locality number is the right-hand number. The groups are (B) younger alluvium, (C) older alluvium, (D) sand over basalt, (E) dry lake sediments, (F) olivine basalt flow of spectral type 2, (G) olivine basalt flow of spectral type 1, (H) olivine basalt flow of spectral type 3. In addition, there are (A) rock standard granodiorite and (I) rock standard gabbro. The discriminant program operates in a stepwise manner to find the most powerful discriminant in  $X$ -dimensional space, where  $X$  is the number of spectral emittance values as sequentially selected by the program (3).
12. S. J. Garawicki is quoted [in L. F. Dellwig, *Modern Geology* (Gordon & Breach, New York, 1969), p. 63; see also pp. 72-73] as follows, "playa surface (dry lake sediments) is a hard dense compact argillic crust consisting of approximately 79% clay, 20% granular components, 0.2% accessory minerals and a trace of saline minerals."
13. J. D. Friedman [*U.S. Geol. Surv. Tech. Lett. NASA-20* (1966), p. 4] gives the composition of the basalt flows at Pisgah Crater: (flow II) total feldspar 15.4 percent and total ferromagnesian 9.4 percent; (flow III) total feldspar 38.8 percent and total ferromagnesian 5.1 percent. Flow III is more spathic than flow II, at least at the two points sampled near the crater. Herein lies one of the major problems in relating regionally variable (airborne) composition data to those of classical geological studies, which are usually from selected points.
14. See note 3 in (7). Standard rock I: gabbro, contains plagioclase (60 percent anorthite molecule content), augite, and a little biotite; standard rock A, granodiorite, contains biotite, quartz, epidote, and plagioclase with orthoclase.
15. The marked drop-off near 8  $\mu\text{m}$  (in Fig. 2E) or the correspondingly high maxima at 8.8  $\mu\text{m}$  may be due to the Christiansen effect in these fine-grained materials. This, however, does not fit for the lavas (Fig. 2, F and G).
16. The 24-channel scanner [E. M. Zaitzeff, C. L. Korb, C. L. Wilson, *Inst. Electr. Electron. Eng. Trans. GE-9*, 114 (1971)] has six channels selected within the thermal band, as CH 16 (6.0 to 7.0  $\mu\text{m}$ ), CH 17 (8.3 to 8.8  $\mu\text{m}$ ), CH 18 (8.8 to 9.3  $\mu\text{m}$ ), CH 19 (9.3 to 9.8  $\mu\text{m}$ ), CH 20 (10.1 to 11.0  $\mu\text{m}$ ), CH 21 (11.0 to 12.0  $\mu\text{m}$ ), and CH 22 (12.0 to 13.0  $\mu\text{m}$ ). The data in (I) would represent the combination of channels 17 to 20, ratioed with the combined channels 19 to 21. My spectral data (Fig. 2) indicate that the Pisgah geology would be more clearly defined by using channels 17, 18, and 19 (either singly or combined), ratioed to channel 20. Channel 21 would still show some effect of chemical compositions (particularly in femic rocks).
17. This research was supported in its entirety by NASA contract NAS9-7313 with NASA/MSC, Houston. This financial support is gratefully acknowledged. This is Technical Report No. 71-5, Remote Sensing Laboratory, Stanford University.

21 September 1971, revised 22 November 1971

## Rock-Type Discrimination from Ratioed Infrared Scanner Images of Pisgah Crater, California

**Abstract.** *The radiances in two thermal infrared channels of an airborne scanner system were ratioed to produce images that recorded compositionally diagnostic emittance variations for several silicate rock types near Pisgah Crater, California.*

One of the recognized objectives of geological remote sensing has been the automatic conversion of scanner data from aircraft or satellites to geologic maps as accurate as those produced with the present techniques employed by field geologists, though on a different scale of spatial resolution. To this end, we have imaged radiance ratios of two spectral channels of data from a thermal infrared scanner that were collected during a flight over Pisgah Crater, California. We believe that these ratio images, which simultaneously record spectral and spatial information, indicate compositional differences among several types of silicate rock in the area. Data from the Pisgah Crater area, gathered by Lyon (1), who used an airborne infrared spectrometer, agree with ours on the spectral characteristics of the regions common to both investigations.

Silicate rocks display reststrahlen bands (departures of the spectral emittance from a value of 1.0) in the wavelength region from 8 to 12  $\mu\text{m}$ , and the positions of these bands, as well as their spectral shapes, vary from silicate to silicate (2, 3). The only chemical parameter that has been experimentally related to the position of the reststrahlen wavelength has been  $\text{SiO}_2$  content (4), though the correlation is crude. The relationship, greatly simplified, is that generally the reststrahlen positions occur at longer wavelengths for rocks containing less  $\text{SiO}_2$ .

Instead of measuring the shapes and positions of the reststrahlen bands with narrow-band spectrometers, as Lyon and Patterson (5) did, we monitored the reststrahlen features by ratioing the radiances detected in two medium-width ( $\Delta\lambda \approx 2.5 \mu\text{m}$ ) spectral channels, in which sufficient energy is collected

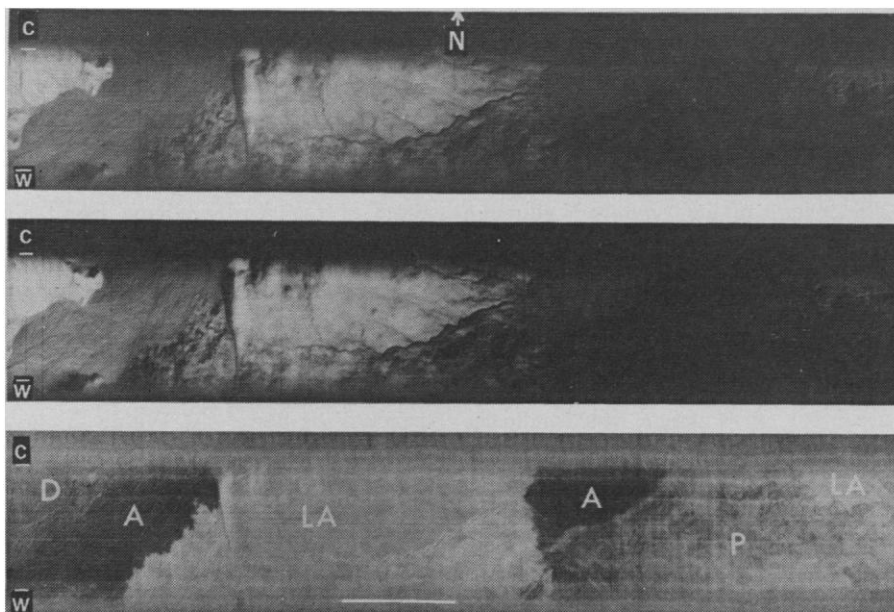


Fig. 1. Analog infrared images of the first section of a west-to-east flight line about 5 miles south of Pisgah Crater (1 mile = 1.6 km). North is toward the top. The channel 1, channel 2, and ratio  $R_{12}$  images are at the top, middle, and bottom, respectively. From left to right, the warm (bright in single-channel images) region in the westernmost part is a dacitic mountain (D); the adjacent colder region is alluvium (A), which grades eastwardly to small rock fragments and sand; and the broad, warm region is the basaltic Sunshine lava flow (LA). Just east of the lava flow is more alluvium (A), followed by playa deposits (P), which are mostly clay, and the southern tip of the basaltic Pisgah Crater lava flow (LA). The approximate edges of the cold and warm calibration plates are marked C and W, respectively. This scale is 0.5 mile per inch.